

UDC 541.182.

*K. Kaneko*¹, *Y. Iizuka*¹, *Y. Ujihara*¹, *T. Hashishin*², *T. Hanasaki*¹

ELECTRORHEOLOGICAL PROPERTIES OF LIQUID CRYSTALLINE GOLD NANOPARTICLES IN A NEMATIC SOLVENT

¹Department of Applied Chemistry, College of Life Sciences, Ritsumeikan University,
1-1-1, Nojihigashi, Kusatsu, Shiga 525-8577, Japan

²Graduate School of Science and Technology, Kumamoto University,
2-39-1 Kurokami, Chuo-ku, Kumamoto 860-8555, Japan

E-mail : kaneko@fc.ritsume.ac.jp. E-mail : hanasaki@sk.ritsume.ac.jp

The electrorheological (ER) properties of a composite material consisting of a nematic liquid crystal (LC) and gold nanoparticles covered with mesogenic groups are studied. The gold nanoparticles are covered by normal alkyl chains and LC compounds. The miscibility of the gold nanoparticles with the nematic LC is investigated by polarizing optical microscopy (POM). In order to improve the ER effect of the composite, a simple strategy is investigated from the viewpoint of a material design in surface-modified gold nanoparticles by a lateral substitution of the mesogenic groups. The presence of the gold nanoparticles in the nematic LC leads to the slight enhanced ER effect compared to that observed for 5CB. This study demonstrates the potential of a hybrid system consisting of LCs and gold nanoparticles to yield a larger ER effect.

Key words : electrorheology, side-on interactions, nematic, nanoparticles.

DOI: 10.18083/LCAppl.2017.2.28

*K. Kaneko*¹, *Y. Iizuka*¹, *Y. Ujihara*¹, *T. Hashishin*², *T. Hanasaki*¹

ЭЛЕКТРОРЕОЛОГИЧЕСКИЕ СВОЙСТВА ЖИДКОКРИСТАЛЛИЧЕСКИХ НАНОЧАСТИЦ ЗОЛОТА В НЕМАТИЧЕСКОМ РАСТВОРИТЕЛЕ

¹Department of Applied Chemistry, College of Life Sciences, Ritsumeikan University,
1-1-1, Nojihigashi, Kusatsu, Shiga 525-8577, Japan

²Graduate School of Science and Technology, Kumamoto University,
2-39-1 Kurokami, Chuo-ku, Kumamoto 860-8555, Japan

E-mail : kaneko@fc.ritsume.ac.jp. E-mail : hanasaki@sk.ritsume.ac.jp

Изучены электрореологические (ЭР) свойства композитного материала, состоящего из нематического жидкого кристалла (ЖК) и наночастиц из золота, покрытых мезогенными группами.

Наночастицы золота покрыты алкильными цепями и ЖК-веществом. С помощью поляризационной оптической микроскопии (ПОМ) изучены смешиваемость наночастиц золота с нематическим ЖК. С целью увеличения ЭР-эффекта композита исследована простая стратегия, связанная с дизайном материала на основе поверхностно-модифицированных наночастиц золота при латеральном замещении мезогенных групп. Наличие наночастиц золота в нематическом ЖК приводит к небольшому усилению ЭР-эффекта по сравнению с эффектом, наблюдавшимся в чистом 5-СВ. Данное исследование показывает потенциал гибридной системы, состоящей из ЖК и наночастиц золота, с целью получения большего ЭР-эффекта.

Ключевые слова: электрореология, боковые взаимодействия, нематик, наночастицы.

Introduction

Electrorheological (ER) effect is the term used to the phenomenon in which the viscosity of fluids is changed by the application of electric fields. To date, there have been many experimental and theoretical studies of both their fundamental and their practical applications [1–10] since the first investigation of the phenomenon by Winslow [11]. ER fluids are mainly divided into two types on the basis of the component of the fluids and the mechanism of the effect. One is the heterogeneous ER fluid in which the particles with large polarization induced by an external electric field are suspended in insulating oil. The other is called the homogeneous ER fluid predominantly composed of an organic polar liquid having a spontaneous polarization such as liquid crystals (LCs). It has been found that the ER fluids have great potential in a number of actuator devices and robotics such as brakes, clutches and dampers in motor vehicles. The magnitude of the electric-field-induced shear stresses that are achievable with fluids presently available is of order kilopascals for fields of order kilovolts per millimeter. However there are still highly vital problems to be solved for extensive commercial uses of the ER fluids because of sedimentation of the particles, abrasion of the surface of the plates with the particles by repeating the application, high voltage, slow rise and decay time and so on.

To integrate and hybridize both types of the ER fluids would lead to new fused materials with higher performance in addition to each intrinsic potential for yielding generated shear stresses. We have reported that the composite consisting of a nematic LC (4'-pentyl-4-biphenylcarbonitrile, 5CB) and the gold

nanoparticles with alkyl chains and mesogenic groups showed a higher enhancement in the shear stress under an application of electric fields [12]. In the system, the enhanced shear stress could be accounted by the assumption that the LC moieties show resistance to the shear flow and the particles enhance the viscosity change caused by the bridged structure between the electrodes under an applied electric field. Furthermore, the surface modification of the gold nanoparticles was found to be very important for tuning the miscibility with 5CB.

The main objective of this study is to develop the ER effect of a composite material consisting of gold nanoparticles covered by LC molecules and a nematic LC (5CB). In order to improve the ER effect of the composite, a simple strategy was investigated from the viewpoint of a material design in surface-modified gold nanoparticles. A lateral substitution of mesogenic groups onto nanoparticles has proven quite effective in emergence of liquid crystallinity [13–15]. There have been some literatures showing nematic phases, smectic phases and columnar phases for LC gold nanoparticles, however the number of those that exhibit LC behavior is still limited among the studies on nanoparticles functionalized with aliphatic chains and LC groups [13–26].

Herein, we show the ER effect of the gold nanoparticles in the nematic LC as a function of the shear rate. It is also demonstrated how the gold nanoparticles behave under an applied electric field by polarizing optical microscope (POM) observations. The structure of the gold nanoparticle covered with normal alkyl chains and the LC molecules in lateral attachment is shown in Fig. 1.

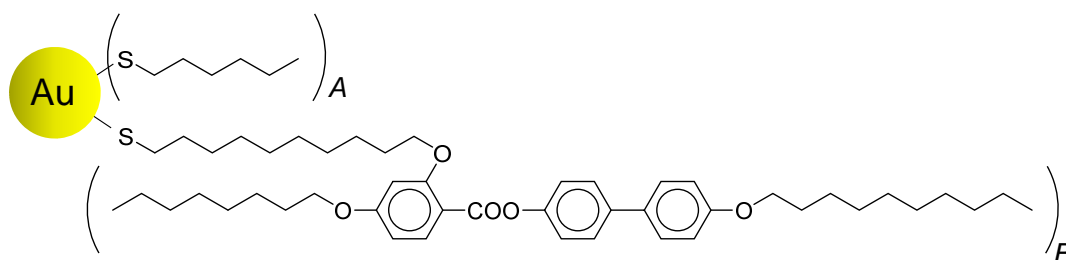


Fig. 1. Molecular structure of the liquid crystalline gold nanoparticles (GNP-C6-8-3R-10). The mesogenic groups were connected by "side-on" attachment

Experimental

Materials. 1,10-Dibromodecane, 4'-hydroxy-4-carbonitrile, 1-decanethiol, and 1-hexanethiol were purchased from Tokyo Kasei Kogyo Co., Ltd. All solvents in this study were used without further purification.

Characterization. $^1\text{H-NMR}$ measurements were performed with a JEOL ALPHA-400 FT NMR (400 MHz) spectrometer using CDCl_3 and deuterated DMSO solvents. Thermal properties were measured by differential scanning calorimetry (DSC) using a Diamond DSC (Perkin Elmer) with heating and cooling rates of $5\text{ }^\circ\text{C}\cdot\text{min}^{-1}$. The textures of the LC phases were observed with a Nikon Eclipse E600 polarizing optical microscope (POM) equipped with a Mettler Toledo FP-82 hot stage and a Mettler Toledo FP-90 central processor.

Rheological Measurements. The rheological properties were measured on a rotational rheometer (Rheosol-G2000, UBM Ltd.) equipped with an electric-field controller (Matsusada Precision Devices, high voltage supply). All the measurements were performed using 15 mm diameter parallel plates and a 0.1 mm gap. The sample was first mounted between the parallel plates, heated to the isotropic state, and held at this temperature for 10 min. It was then allowed to cool to the measuring temperature and allowed to equilibrate for 10 min. An electric field of 3 kV mm^{-1} was applied between the upper and lower plates under steady shear flow and constant shear rate. The generated shear stress was defined as the difference between the shear stress measured in the presence and absence of the electric field.

Results and Discussion

Characterization by $^1\text{H NMR}$ and TEM

The gold nanoparticles covered by normal alkyl chains and LC thiol compounds (8-3R-10) were characterized by $^1\text{H NMR}$ spectroscopy. The broadening of the peaks is one of the evidences for the coverage of the gold nanoparticles by the alkyl chains and the LC thiol compounds. The detail synthetic manner is referred in our previous paper [12].

LC thiol compound (8-3R-10)

$^1\text{HNMR}$ (CDCl_3) δ : 8.04 (d, $J=19.0\text{ Hz}$, 1H), 7.57 (d, $J=24.5\text{ Hz}$, 2H), 7.51 (d, $J=23.1\text{ Hz}$, 2H), 7.22 (d, $J=12.7\text{ Hz}$, 2H), 6.97 (d, $J=27.2\text{ Hz}$, 2H), 6.57–6.48 (m,

2H), 4.10–3.95 (m, 6H), 2.47 (q, $J=40.3\text{ Hz}$, 2H), 1.88–1.75 (m, 6H), 1.53–1.19 (m, 44H), 0.96–0.83 (m, 6H).

A high-resolution transmission electron microscopy (HR-TEM) image of GNP-C6-8-3R-10 is shown in Fig. 2. The HR-TEM image depicts the aggregate of LC thiol-capped GNP-C6-8-3R-10 in the size of 40–60 nm, which was composed of single Au nanoparticles with an average diameter of $2.5\pm 1.0\text{ nm}$. The size also was in good agreement with the size of other LC thiol-capped Au nanoparticles [12].

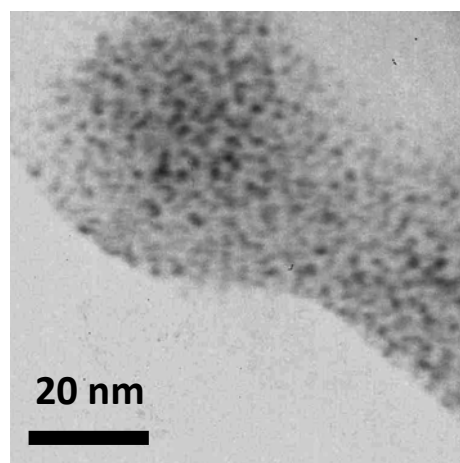


Fig. 2. HR-TEM image of the gold nanoparticles (GNP-C6-8-3R-10)

Phase transition behavior

The phase transition behavior of the thiol compound (8-3R-10) and the gold nanoparticle (GNP-C6-8-3R-10) was studied by DSC and POM observations. The thiol compound (8-3R-10) exhibited a Schlieren texture in a temperature range from 29.0 to 64.0 $^\circ\text{C}$ on heating from the crystal state (scanning rate: $5\text{ }^\circ\text{C min}^{-1}$) as shown in Fig. 3, *a*. In the DSC diagram in Fig. 4, an endothermic peak was detected at 28.9 $^\circ\text{C}$. This temperature is in good agreement with that at which the texture appeared in the POM observation on heating. This result was related to the appearance of the nematic phase. An additional endothermic peak was observed at 64.0 $^\circ\text{C}$ on heating, which corresponds to the clearing point.

From the POM observation, GNP-C6-8-3R-10 was found to exhibit liquid crystallinity. The DSC curves of GNP-C6-8-3R-10 are shown in Fig. 4. They displayed the baseline shifts on both heating and cooling, which was assigned to the glass transition, and the peaks corresponding to the clearing point (around 130 $^\circ\text{C}$). A Schlieren-like texture was observed

in a temperature range below the clearing point under POM. This texture is a typical characteristic of a nematic phase.

Several studies on grafting mesogenic groups onto gold nanoparticles have been performed. A nematic phase was obtained by Mehl *et al.*, [13–15] whereas a cubic phase was observed by Donnio *et al.*, [18] and a smectic phase and a columnar phase by Gorecka *et al.* [22, 23]. The lateral attachment of the mesogenic groups onto the gold nanoparticles was found to be effective to emerge the LC organization. It

can be deduced that the laterally attached mesogenic groups play an essential role in the formation of the mesophase. This effect is associated with the whole topology of the particle. The side-on attachment would provide a cylindrical molecular shape, which resulted in the appearance of LC-phases. The wider LC temperature range of GNP-C6-8-3R-10 is due to the larger domains of the gold nanoparticles covered with the mesogenic groups, and the thermal stability was consequently promoted compared with the corresponding mesogenic groups.

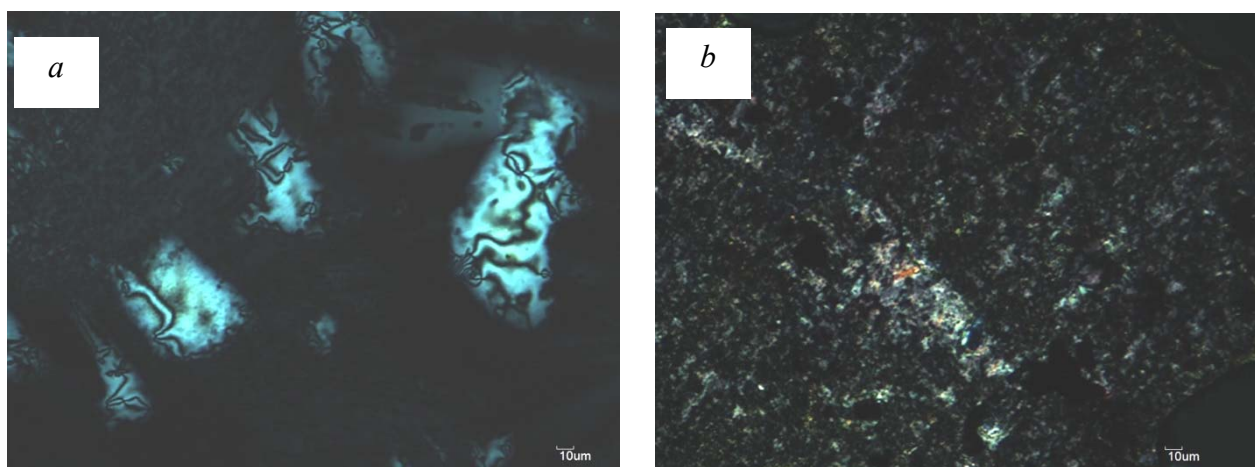


Fig. 3. POM images of (a) the thiol mesogen (8-3R-10) and (b) the gold nanoparticles (GNP-C6-8-3R-10) on heating

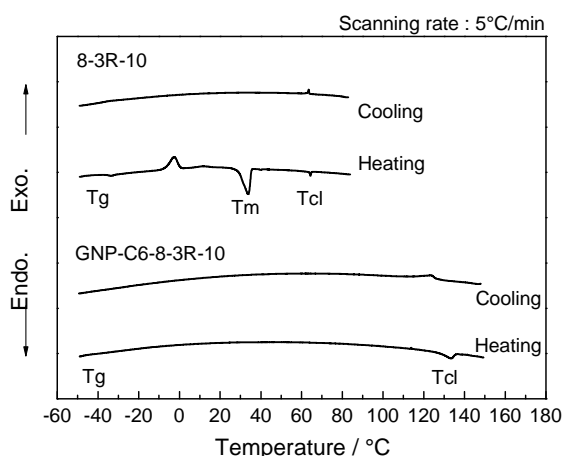


Fig. 4. DSC curves of the thiol mesogen (8-3R-10) and the gold nanoparticles (GNP-C6-8-3R-10)

Electrorheological properties

The response of the composite under an electric field was investigated by steady shear experiments. An electric field was repeatedly applied to the composite, at

intervals of 100 s. The rheological results for 5CB and the composite [GNP-C6-8-3R-10 (10 wt. %) in 5CB] at a constant shear rate of 100 s^{-1} are shown in Fig. 5. The steady states were obtained without an electric field for both samples, where the shear stress of the composite was higher than that of 5CB due to the high viscosity of GNP-C6-8-3R-10. After the application of an electric field for 100 s, the shear stresses of the two samples increased immediately. A smooth decrease in shear stress was also observed after the removal of the electric field, which indicates that the organized structures could relax to their initial state. The reversibility of the system is demonstrated by the rapid relaxation of the rheological properties upon the removal of the electric field. Multiple cycles of the electrorheological response can be observed at a shear rate of 100 s^{-1} , which is indicative of the stable repeatability of the ER effect. On the basis of the results obtained, the generated shear stress in the composite was slightly enhanced by the addition of the gold nanoparticles.

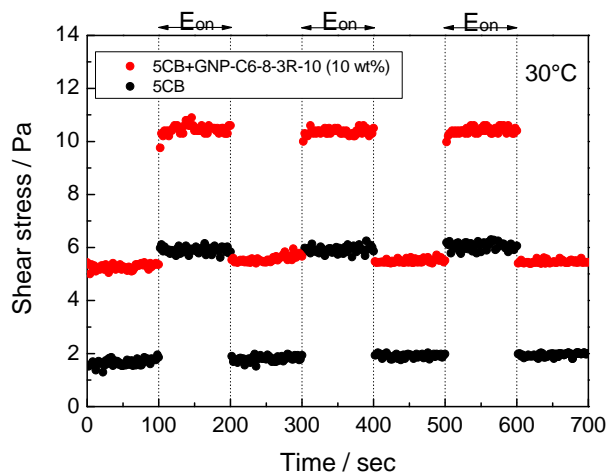


Fig. 5. ER responses of 5CB and the composite (GNP-C6-8-3R-10 (10 wt. %) in 5CB) under 3 kVmm^{-1}

The dependence of the shear rate on the shear stress of the composite (10 wt. %) at 30°C is shown in Figure 6.

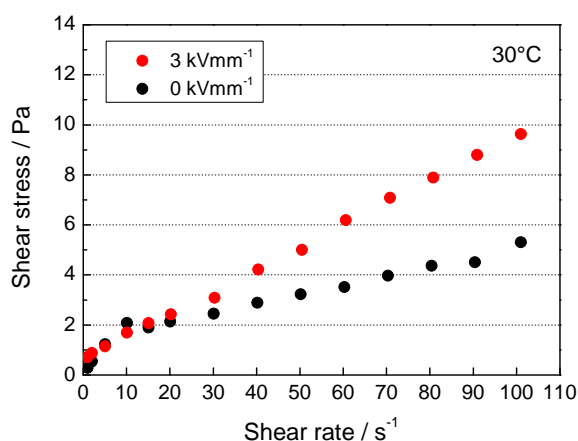


Fig. 6. Shear stress as a function of shear rate of the composite [GNP-C6-8-3R-10 (10 wt. %) in 5CB] under 0 and 3 kVmm^{-1}

With regards to the measurement of the shear stress as a function of the shear rate, we should mention that the shear stress was measured by increasing the shear rate stepwise from 0 to 100 s^{-1} . As shown in Fig. 6, the shear stresses increased roughly in proportion to the shear rate under 0 and 3 kVmm^{-1} , which is known as Newtonian behavior. This is mainly originated by 5CB, which is categorized in homo-

geneous ER fluids. Generally, Bingham behavior is observed in heterogeneous ER fluids in which the viscosity change occurs owing to a crosslinked structure of the particles under an electric field. This would be caused by the fact that the particle size of GNP-C6-8-3R-10 contained in the composite is extremely small, and then the crosslinked structure is easily destroyed by Brownian motion of 5CB molecules.

POM observation under an applied electric field

The compositional homogeneity of the produced composite is an important step towards the application of LC-based ER fluid devices. The miscibility of GNP-C6-8-3R-10 to 5CB was accurately evaluated by the POM observation. Optical investigations of the composite under an applied electric field were carried out in a transparent sandwich-type cell consisting of two glass plates coated with indium tin oxide (ITO) and treated for a homogeneous alignment. The composite was induced into the cell at the isotropic state (50°C) and then cooled to the temperature at which the ER measurement was performed (30°C). The POM images of the composite are shown in Fig. 7, *a-d*, respectively. A microaggregation of the gold nanoparticles in 5CB was apparently observed as shown in Fig. 7, *a*. Next, the alignment behavior of the composite was observed when an electric field was applied. The POM image shown in Fig. 7, *b* turned dark upon the application of an electric field perpendicular to the ITO surface. This implies that 5CB molecules were homeotropically aligned along the direction of the electric field. Thus, the alignment of 5CB was unaffected by the macroscopic aggregation of GNP-C6-8-3R-10.

Subsequently, in order to confirm the behavior of the particles under an electric field, the POM observation was conducted under open Nicol. Fig. 7, *c* and 7, *d* shows the POM images of the composite under 0 and 3 kVmm^{-1} , respectively. As can be seen from the figures, the composite had the microaggregation in the absence of electric field and no change in the aggregation occurred even after the application of the electric field. From the results of the POM observation and the ER measurements, it could be concluded that the crosslinked structure of the particles rarely played an effective role in the enhanced ER effect.

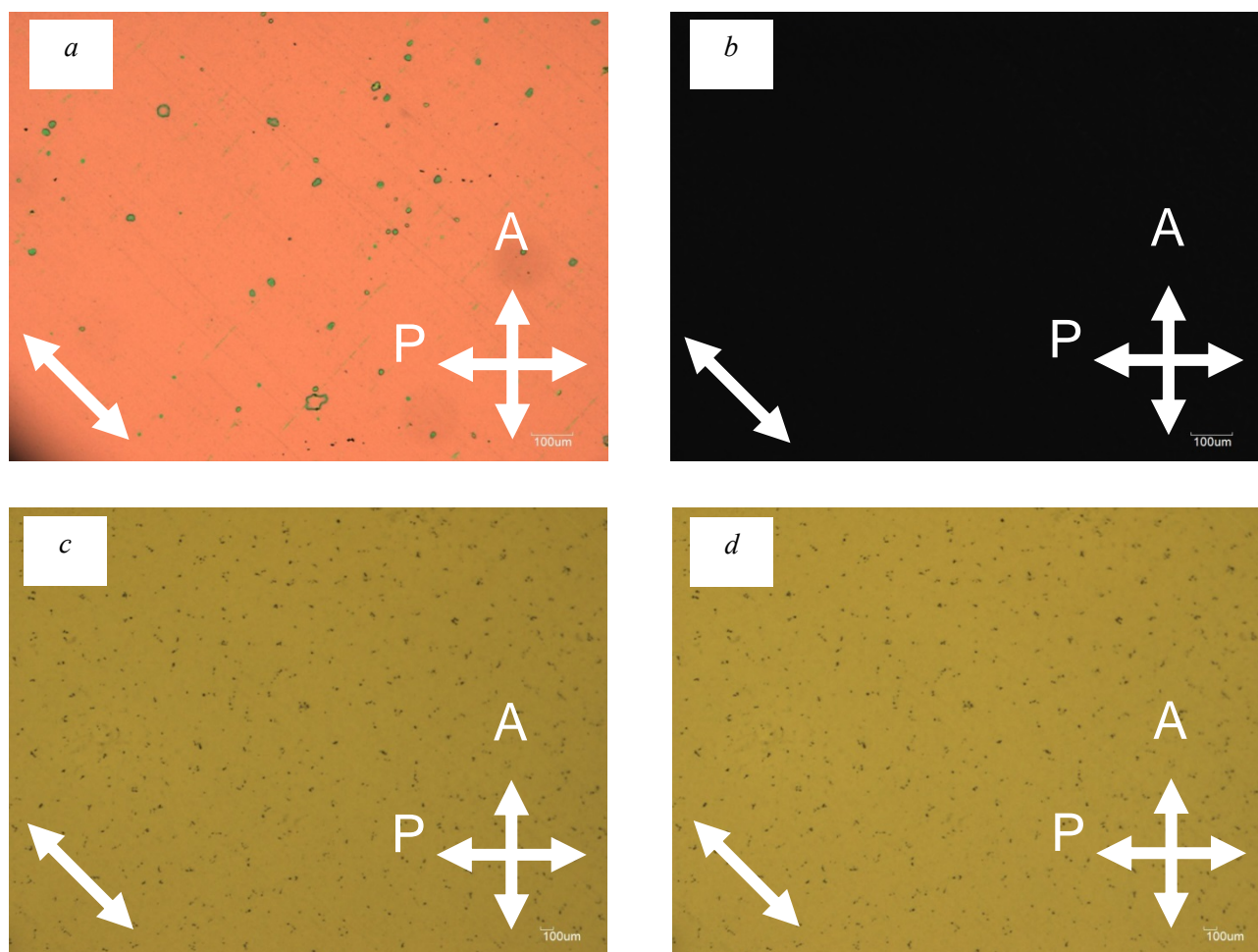


Fig. 7. (a), (b) – Cross and (c), (d) – open Nicol images of GNP-C6-8-3R-10 (10 wt. %) in 5CB at 30 °C. The images were taken under (a), (c) 0 kVmm⁻¹ and (b), (d) 3 kVmm⁻¹, respectively

Conclusion

To conclude, we presented the fabrication of the LC gold nanoparticles and the ER effect of the composite consisting of the LC gold nanoparticles and the nematic LC. By adding the LC gold nanoparticles into 5CB, the slight enhanced change in the shear stress for the LC composite was observed compared with that observed for only 5CB. Our approach in which the mesogenic groups were laterally attached onto the gold nanoparticles has successfully provided the emergence of the LC organization and resulted in the fusional ER system by the organic/inorganic materials. Further investigation of the ER properties of such hybrid ER fluids is necessary for yielding larger viscosity changes.

This work was partially supported by a Grant-in-Aid for Challenging Exploratory Research (№ 24656020) from the Japan Society for the Promotion of Science (JSPS) and a MEXT-supported Program for the Strategic Research Foundation at Private Universities (2012-2016).

References

1. Inoue A., Maniwa S. Electrorheological effect of liquid crystalline polymers. *J. Appl. Polym. Sci.*, 1995, **55**, 113–118.
2. Inoue A., Ide Y., Oda H. Influence of dilution by polydimethylsiloxane on electrorheological effect of side-chain liquid crystalline polysiloxane. *J. Appl. Polym. Sci.*, 1997, **64**, 1319–1328.
3. Inoue A., Maniwa S., Ide Y. Relation between molecular structure and electrorheological effects in liquid crystalline polymers. *J. Appl. Polym. Sci.*, 1997, **64**, 303–310.

4. Tanaka K., Oiwa Y., Akiyama R., Kubono A. Shear Thinning and Electro-Rheological Effect for Neat Liquid Crystalline Polysiloxane in the Vicinity of Isotropic-Liquid Crystalline Phase Transition. *Polym. J.*, 1998, **30**, 171–176.
5. Orihara H., Kawasaki T., Doi M., Inoue A. Immiscible polymer blend electrorheological fluids: Composition dependence. *J. Appl. Polym. Sci.*, 2002, **86**, 3673–3680.
6. Mimura K., Nishimoto Y., Orihara H., Moriya M., Sakamoto W., Yogo T. Synthesis of Transparent and Field-Responsive BaTiO₃ Particle/Organosiloxane Hybrid Fluid. *Angew. Chem. Int. Ed.*, 2010, **49**, 4902–4906.
7. Kaneko K., Kawai T., Nakamura N. Electrorheological Effect of “Side-on” Liquid Crystalline Polysiloxane. *ChemPhysChem.*, 2008, **9**, 2457–2460.
8. Kaneko K., Mandai A., Heinrich B., Donnio B., Hanasaki T. Electric Field-Induced Reversible Viscosity Change in Columnar Liquid Crystal. *ChemPhysChem.*, 2010, **11**, 3596–3598.
9. Hanasaki T., Kamei Y., Mandai A., Uno K., Kaneko K. Phase Transition Behavior and Electro-Rheological Effect of Liquid Crystalline Siloxane Dimers. *Liq. Cryst.*, 2011, **38**, 841–848.
10. Kaneko K., Oto K., Kawai T., Choi H., Kikuchi H., Nakamura N. Electro-Rheological Effect and Electro-Optical Properties of Side-on Liquid Crystalline Polysiloxane in a Nematic Solvent. *ChemPhysChem.*, 2013, **14**, 2704–2710.
11. Winslow W. M. Induced Fibration of Suspensions. *J. Appl. Phys.*, 1949, **20**, 1137–1140.
12. Kaneko K., Ujihara Y., Oto K., Hashishin T., Hanasaki T. Electric-Field-Induced Viscosity Change of a Nematic Liquid Crystal with Gold Nanoparticles. *ChemPhysChem.*, 2015, **16**, 919–922.
13. Cseh L., Mehl G.H. The Design and Investigation of Room Temperature Thermotropic Nematic Gold Nanoparticles. *J. Am. Chem. Soc.*, 2006, **128**, 13376–13377.
14. Cseh L., Mehl G.H. Structure-property relationships in nematic gold nanoparticles. *J. Mater. Chem.*, 2007, **17**, 311–315.
15. Zeng X., Liu F., Fowler A.G., Ungar G., Cseh L., Mehl G.H., Macdonald J.E. 3D Ordered Gold Strings by Coating Nanoparticles with Mesogens. *Adv. Mater.*, 2009, **21**, 1746–1750.
16. Kanayama N., Tsutsumi O., Kanazawa A., Ikeda T. Distinct thermodynamic behaviour of a mesomorphic gold nanoparticle covered with a liquid-crystalline compound. *Chem. Commun.*, 2001, 2640–2641.
17. Qi H., Hegmann T. Formation of periodic stripe patterns in nematic liquid crystals doped with functionalized gold nanoparticles. *J. Mater. Chem.*, 2006, **16**, 4197–4205.
18. Donnio B., García-Vázquez P., Gallani J.-L., Guillon D., Terazzi E. Dendronized Ferromagnetic Gold Nanoparticles Self-Organized in a Thermotropic Cubic Phase. *Adv. Mater.*, 2007, **19**, 3534–3539.
19. Marx V.M., Girgis H., Heiney P.A., Hegmann T. Bent-core liquid crystal (LC) decorated gold nanoclusters: synthesis, self-assembly, and effects in mixtures with bent-core LC hosts. *J. Mater. Chem.*, 2008, **18**, 2983–2994.
20. Qi H., Kinkead B., Hegmann T. Unprecedented Dual Alignment Mode and Freedericksz Transition in Planar Nematic Liquid Crystal Cells Doped with Gold Nanoclusters. *Adv. Funct. Mater.*, 2008, **18**, 212–221.
21. Qi H., Kinkead B., Marx V.M., Zhang H.R., Hegmann T. Miscibility and Alignment Effects of Mixed Monolayer Cyanobiphenyl Liquid-Crystal-Capped Gold Nanoparticles in Nematic Cyanobiphenyl Liquid Crystal Hosts. *ChemPhysChem.*, 2009, **10**, 1211–1218.
22. Wojcik M., Lewandowski W., Matraszek J., Mieczkowski J., Borysiuk J., Pocięcha D., Gorecka E. Liquid-Crystalline Phases Made of Gold Nanoparticles. *Angew. Chem. Int. Ed.*, 2009, **48**, 5167–5169.
23. Wojcik M., Kolpaczynska M., Pocięcha D., Mieczkowski J., Gorecka E. Multidimensional structures made by gold nanoparticles with shape-adaptive grafting layers. *Soft Matter.*, 2010, **6**, 5397–5400.
24. Draper M., Saez I.M., Cowling S.J., Gai P., Heinrich B., Donnio B., Guillon D., Goodby J.W. Self-Assembly and Shape Morphology of Liquid Crystalline Gold Metamaterials. *Adv. Funct. Mater.*, 2011, **21**, 1260–1278.
25. Nealon G.L., Greget R., Dominguez C., Nagy Z.T., Guillon D., Gallani J.-L., Donnio B. Liquid-crystalline nanoparticles: Hybrid design and mesophase structures. *Beilstein J. Org. Chem.*, 2012, **8**, 349–370.
26. Mischler S., Guerra S., Deschenaux R. Design of liquid-crystalline gold nanoparticles by click chemistry. *Chem. Commun.*, 2012, **48**, 2183–2185.

Поступила в редакцию 17.05.2017 г.
Received 17 May 2017